Visualizing Relativistic Effects in Spacetime

Ping-Kang Hsiung*
Robert H. P. Dunn†
Carnegie Mellon University
Pittsburgh, Pennsylvania 15213

Abstract

We have developed an innovative ray-tracing algorithm to describe *R*elativistic *E*ffects in *S*pace*T*ime ("REST"). Our algorithm, called *REST-frame*, simulates a generalized world in Spacetime and gives the fine details implicit in the Special Theory of Relativity that have not yet been made apparent. These novel simulations disclose the non-intuitive realm of Special Relativity and, by visualization means, advance beyond the findings of past revelations concerning relativistic effects.

Through the application of state-of-the-art computation technology and simulation techniques to earlier quests in Physics, REST-frame offers a flexible visualization tool to study some of the most exciting aspects of the natural world; particularly, the rich visual properties associated with the finite speed of light.

Keywords: Apparent effects of Special Relativity. Scientific visualization. Computer image synthesis. Ray-tracing. Computer simulation.

1 Introduction

1.1 Motivations

The revival of interest in Special Relativity in the early 1960's was focused on the appearance of relativistic objects under *ad hoc* conditions. Until that time, for nearly fifty-five years since the inception of the special theory, such phenomena had not been fully explored. The nature of the revival itself was limited in that scientists lacked the computing power, ray-tracing techniques, and visualization outlook.

Our intent today is to simulate and visualize real world representations of Special Relativistic effects by the application of an innovative ray-tracing algorithm.

*Department of Electrical and Computer Engineering, Carnegie Mellon University. (412) 268-2524. pkh@vap.vi.ri.cmu.edu

†Department of Art, Carnegie Mellon University.

This research was partially supported by Imaging Systems Laboratory, The Robotics Institute, Carnegie Mellon University.

1.2 Background

Einstein's Special Theory of Relativity (1905) postulated [26][32][19]:

1. Non-existence of preferred reference system (*"The Principle of Relativity"*): the laws of physics must be the same for observers in all inertial reference systems.[1]
2. Constancy of speed of light: c is constant in a vacuum in all inertial frames and is independent of the motion of a light source relative to the observer.

Some consequences of the Spacetime model are:

- The measured space and time coordinates are dependent upon the reference frame from which the measurement is conducted.
- The Lorentz Transformation equations relate measured Spacetime coordinates between inertial reference frames.
- Lengths perpendicular to relative motion remain the same measurements regardless of the inertial observer.
- Lengths parallel to relative motion are measured to have undergone contraction in comparison with their rest lengths.
- Clocks in inertial frames have varying rates dependent upon their motion.

Ray-tracing synthesizes images using a model that reverses the image formation process in nature [15][1] (figure (1)). Rays are traced from pixels on the image plane through a fixed "eye-point" (or "viewpoint") into the object space that forms the scene. The light intensity of the rays contributes to the final pixel intensity of the synthesized image. Reflection and refraction rays are recursively generated when rays meet (*"hit"*) objects. This ray-tracing computation can be modeled as two interacting processes: the *intersection process* and the *shading process* (figure (2))[16]. The former solves intersection points where rays hit scene object surfaces, and the latter performs shading computations according to some illumination model, e.g. Phong[25], Whitted[37], Torrance-Sparrow[35], or Cook-Torrance[8].

[1] A reference system, or *reference frame*, is *inertial* in Spacetime if it is nonaccelerating.

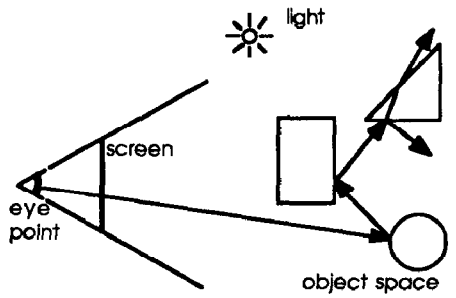

Figure 1: Ray-tracing principle

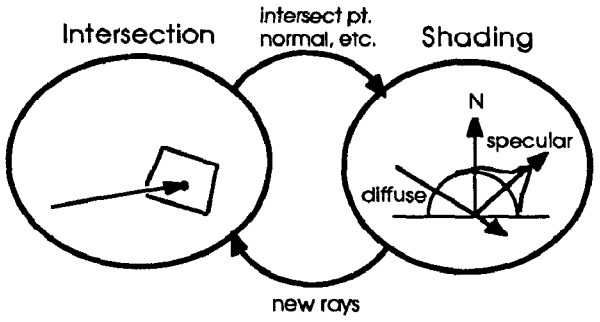

Figure 2: Ray-tracing computation model

1.3 Previous work

James Terrell (1959)[33] made an early distinction between the *appearance* or visibility of relativistic effects and the *measurement* of relativistic effects. Following the initial work of Penrose (1959)[24] and Terrell, interest was sparked and a number of related papers were published[36][31][5][27][40][30][20][29][12].

The following work is of particular interest for our purposes: Sten Yngström (1962)[40] established the aberration formula and a general expression for the apparent shape of a moving body for the cases of observation by sight and by radar (photography with flash lighting). Scott and Viner (1965)[30] considered the appearance of a relativistic plane grid and a relativistic group of boxes in perspective. They presented the composite result of the classical Doppler effect[2] and the relativistic Lorentz-Fitzgerald contraction. Penrose[24] and Scott and van Driel[29] studied the appearance of relativistically moving spheres. The objects under consideration were assumed to be self-luminous or continuously and uniformly illuminated.

Their work is incomplete because *ad hoc* viewing conditions were always assumed and the subject was treated as a conformal-mapping of points between coordinate systems. Selected points on objects were mapped (transformed) and interpolations of the transformed points were made to show object outlines. Neither optical effects nor object surface details were reproduced.

Ray-tracing is a rich and well-developed simulation technique[37][1][4]. Recent research focuses on modeling more complex optical and natural phenomena and dynamic systems[38][34][6][39], as well as on improving the computation efficiency through new spatial search algorithms[13][11][17][23][3][7] and multiple-processing[10][2][18][21][22][28]. Previous work related to the time aspects of the ray-tracing algorithm includes Cook et. al's stochastic ray-tracing[9] in creating motion blur and depth-of-field effects, and Glassner's multiple-frame computation acceleration technique[14] that exploits the spatial and temporal coherency of the ray-tracing simulation. To this day, a light ray has always been regarded as if it traveled with infinite speed, and no treatment has yet been given to visualizing the Spacetime world of Special Relativity, in which light has a finite speed.

[2] In their work, this refers to the effect of *finite (non-zero)* "time-of-flight" of light. This is not to be confused with the relativistic Doppler frequency shift, or the *Red-shift*.

2 Approach

The REST-frame technique synthesizes the visual effects in Spacetime by incorporating the finite speed of light in ray-tracing to simulate the Spacetime physical world modeled by Einstein's Special Relativity. Light-rays are traced back to their source events in the *past* in Spacetime from the observation point, which is itself an event-point in Spacetime. The three major elements in our approach are:

- Modeling of time in the ray-tracing equations.
- Lorentz Transformation of rays under Special Relativity.
- Ray-object intersection in Spacetime.

The Doppler effect is implicitly accounted for when the first two elements are formulated correctly in our system.

We will elaborate upon these three elements in steps in the following sections after a short introduction to the Lorentz Transformation formula in Special Relativity and a review of the assumptions used in the ray-tracing technique.

2.1 Lorentz Transformation and the ray-tracing technique

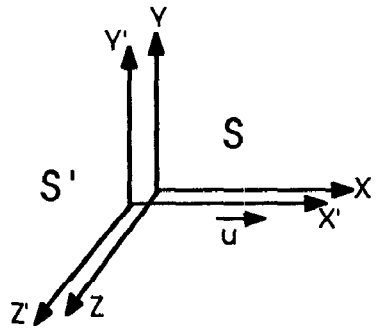

Figure 3: Geometry for Lorentz Transformation derivation

Lorentz Transformation relates the position and time of occurrence of a *single* physical event measured by two observation systems (called *frames*) moving relative to one another. For inertial Cartesian coordinate system S'(x', y', z') with time

t' that travels at speed u relative to system S(x, y, z) and time t along their common X and X' axes (figure (3)), if its Y' and Z' axes coincide with Y and Z, respectively, of S at time $t = t' = 0$, then the measurement of coordinates and times in S' and S are related by

$$\begin{aligned} x' &= \gamma(x - ut), \\ y' &= y, \\ z' &= z, \\ t' &= \gamma(t - \beta\frac{x}{c}) \end{aligned} \qquad (1)$$

in which $\beta = u/c$ and $\gamma = 1/\sqrt{1-\beta^2}$, c being the speed of light. For our convenience, we can normalize c to 1, and write $\beta = u$.

The conventional ray-tracing technique models the classical Galilean-Newtonian physics, in which an infinite light-speed is implicitly assumed, and consequently a notion of global, universal *simultaneity* is taken to exist. A "ray" (*light* ray as it is) in ray-tracing, as defined by its origin $\vec{X_0} = (x_0, y_0, z_0)$ and normalized direction cosine $\vec{a}$,[3] is represented by an unidirectional half-line in 3D in its parametric form:

$$r\vec{a}y_{classical} = (x, y, z) = (x_0, y_0, z_0) + t\,\vec{a} \qquad (t \geq 0) \qquad (2)$$

The parameter t gives the geometric *distance* (in the classical 3D sense) of points on the half-line from the ray origin (x_0, y_0, z_0), and is always a positive number. As t increases from 0, the "ray-front" (x, y, z) moves away in space from its origin in the direction $\vec{a}$. There is no need to express the time information in this ray equation because it is assumed that all rays that form the image, with their infinite space-traveling speed, arrive at the image plane *simultaneously*. Moreover, this time is assumed to be simultaneous with the time the rays underwent the (perhaps more than once) reflection and refraction interactions with the scene objects. The objects remain stationary over the image formation time.[4]

2.2 Time-modeling in Spacetime ray-tracing

When the scene objects and the image plane (or the camera plate) are in relative motion at speeds comparable to light speed, the time information must be interwoven with the spatial coordinates in defining the vision formation process. To model this Spacetime physics correctly, we define the image formation event to take place at the Spacetime event point $[x_0, y_0, z_0, t_0]$[5] in frame S, in which the image plane is stationary in position. A ray that passes $[x_0, y_0, z_0, t_0]$ and travels in 3D spatial direction $\vec{a}$ in S can be modeled as

$$\begin{aligned} r\vec{a}y_{REST} &= (x, y, z) = (x(t_0),\ y(t_0),\ z(t_0)) + c(t_0 - t)\,\vec{a} \\ &\quad (t \leq t_0) \end{aligned} \qquad (3)$$

[3] $\vec{a}$ for *aim*.

[4] The assumption of instantaneous render time is removed in some ray-tracing research to model motion blur, and in general to overcome the temporal aliasing in ray-tracing. The inter-frame transformation used, however, remains Galilean-Newtonian.

[5] We use the symbol (x, y, z) for 3D positional coordinates and $[x, y, z, t]$ for a Spacetime event point. When we designate a specific reference frame S, we use $(x, y, z)_S$ and $[x, y, z, t]_S$. Individually, each component is written with a subscript S (e.g. t_S). We also use $[x_0, y_0, z_0, t_0]_S$ as a shorthand for event $[x(t_0), y(t_0), z(t_0), t_0]$, and $(x_0, y_0, z_0)_S$ for $(x(t_0), y(t_0), z(t_0))$.

The *physical* interpretation of t is the time the ray (traveling at light speed c) passes the coordinates (x, y, z) in S, starting at $[x_0, y_0, z_0, t_0]_S$. The constraint $(t \leq t_0)$ comes from ray-tracing simulation, which *reverse*-synthesizes the image formation process found in nature, and thus traces rays from present time t_0 to past time $t < t_0$.

Another interpretation of equation (3) is that it defines all events (as points in Spacetime) in the *past* that can make it to event $[x_0, y_0, z_0, t_0]_S$ at light speed by taking a given direction $\vec{a}$. This concept can be conveniently illustrated by the Minkowski Spacetime diagram (figure (4)). In this representation, all events that can be connected to event $[x_0, y_0, z_0, t_0]$ by light in Spacetime form a double-cone surface with vertex $[x_0, y_0, z_0, t_0]$. The upper cone defines the future events in time and the lower cone the events of the past. With the constraint $t < t_0$, equation (3) defines all rays that lie on the lower cone in Minkowski space. Each ray points downward and travels into the past from the present time t_0.

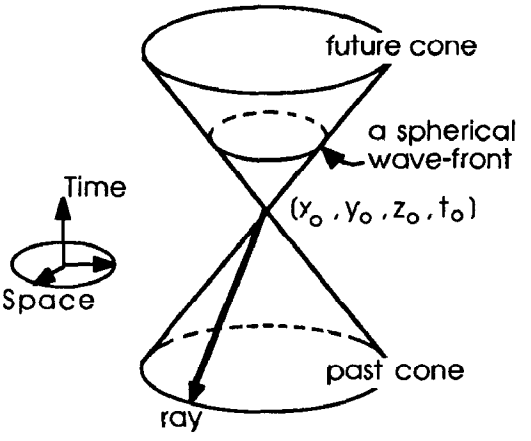

Figure 4: Ray traveling to the past on Minkowski light cones

For the "screen rays" in ray-tracing, $[x_0, y_0, z_0, t_0]$ is the image formation event, with $X(t_0) = (x_0, y_0, z_0)$ being the viewpoint position and t_0 being the image capture time. $\vec{a}$ is the direction of the ray determined by the ray's screen pixel position. For the reflection and refraction rays (the "secondary" rays), $[x_0, y_0, z_0, t_0]$ is the ray-object intersection event, and $X(t_0) = (x_0, y_0, z_0)$ is the 3D point of intersection.

2.3 Translation and rotation of rays

Following from the Special Relativity postulates of

- the non-existence of preferred reference frame, and
- the constancy of light speed in all frames

we can write the S frame ray equation (eq. (3), with c=1) as

$$\begin{aligned} r\vec{a}y'_{REST} &= (x', y', z') = (x'(t'_0),\ y'(t'_0),\ z'(t'_0)) + (t'_0 - t')\,\vec{a}' \\ &\quad (t' \leq t'_0) \end{aligned} \qquad (4)$$

in S' frame, which travels with the objects relative to S in the manner as defined in section 2.1.[6] Furthermore, we can relate

[6] The conditions are: (1) The scene objects, which travel with respect to viewpoint at speed v in X direction, are stationary in S'. (2) The spatial origin in S and S' coincide at time $t = t' = 0$.

corresponding ray equations in S and S' via Lorentz Transformation.

2.3.1 Translation of rays

From Lorentz Transformation, the ray origin event in S' is

$$(x'(t'_0),\ y'(t'_0),\ z'(t'_0)) = (\gamma(x_0 - \beta t_0),\ y_0,\ z_0) \quad (5)$$

$$t'_0 = \gamma(t_0 - \beta x_0) \quad (6)$$

The ray becomes

$$\begin{aligned} \vec{ray'} &= \vec{X'} = (\gamma x_0,\ y_0,\ z_0) - (\gamma\beta x_0 + t')\,\vec{a'} \\ &= (\gamma x_0 - \gamma\beta x_0 a'_x,\ y_0 - \gamma\beta x_0 a'_y,\ z_0 - \gamma\beta x_0 a'_z) \\ &\quad -t'\vec{a'} \end{aligned} \quad (7)$$

A ray thus *appears* to have its origin translated when moving from S to S'. Note that there is a contraction in the direction of the relative motion (X direction).

Since the speed that the ray travels *is* identical (light speed) in both frames according to Special Relativity, we can derive the relativistic aberration equation that relates $\vec{a}$ and $\vec{a'}$ of a light ray to be

$$\vec{a'} = (\gamma(a_x + \beta),\ a_y,\ a_z)/\gamma(1 + \beta a_x) \quad (8)$$

This appears as a rotation of the ray direction going from S to S'.

2.4 Ray-object intersection test

In terms of the ray-object intersection test in ray-tracing computation, equations (7) and (8) allow us to form a ray in the observation frame S and yet perform the ray-object intersection in the S' frame, in which the objects are stationary. This is a special case of the more general situation in which all objects are not traveling in unison. We will discuss this further in section 4.1.

The "time-of-flight" effect (the Doppler effect) is implicitly accounted for in our formulation, as the intersection "points" in REST-frame are in fact past *events* in Spacetime.[7] They are the 3D spatial points that are not only geometrically (optically) visible, in the conventional ray-tracing sense, but also *temporally* visible from the image formation event.

3 Implementation and experiments

3.1 Implementation and experiments set-up

We have chosen to implement this REST-frame ray-tracing approach based on the bounding volume intersection acceleration technique[17].[8]

In our implementation, the scene objects are defined in an input file to the program. Also included in the file are the viewpoint, view time, view angle and view direction parameters. The scene objects are assumed to be stationary in S' frame, which travels, relative to the viewpoint frame S, at a user-specified speed u (which is also β as we have normalized c to 1) in the positive X direction common to both the viewpoint frame and the scene object frame.

Our program fires rays into the past in Spacetime and performs the ray transformation as explained in the previous sections. After a ray hits an object, it spawns reflective and refractive rays according to the surface property of the object. Shadow rays are also cast to all light sources in the scene. The light sources are assumed to be isotropic and stationary in the object S' frame. In order to reduce the computation time of our traces, we do not employ stochastic sampling or anti-aliasing techniques in our current implemenation. We performed our experiments on a DECstation 3100 system with 16M byte of memory. Most of our traces took less than 5 minutes for 512 by 512 images.

3.2 Experimental results

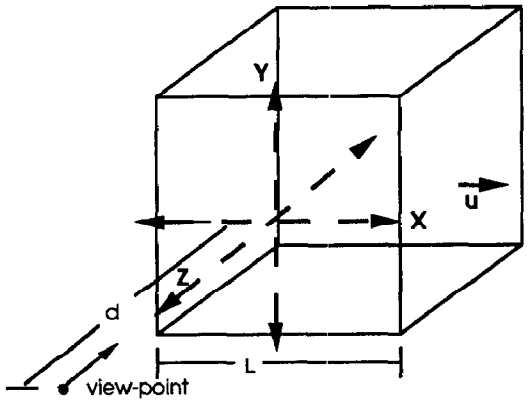

Figure 5: Setup for the contraction calibration experiment

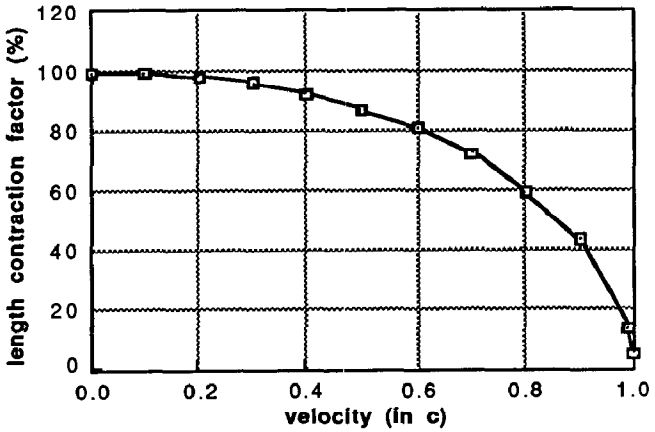

Figure 6: Result of contraction calibration experiment

To verify the correctness of our implementation, we ray-traced a cube with the geometry setup of figure (5). The appar-

[7] With respect to the image formation event.

[8] This this an acceleration scheme for ray-object intersection test in which nested bounding volumes of simple geometries are built around scene objects to form a spatial hierarchy. At ray-tracing time, every ray is tested against the bounding volumes in the hierarchical sequence to identify a subset of objects for more involved ray-object intersection computation.

ent length contraction (the *Lorentz-Fitzgerald Contraction*) of the cube in the X direction was measured[9] as we increased the traveling speed (u) from 0.0 to 0.99 times the speed of light. The result is plotted in figure (6). The length contraction factor that we measured reproduced the formula ($\sqrt{1-\beta^2}$) predicted by Special Relativity.

The second set of experiments has the scene configuration of an 11 x 11 array of bars, each aligned with the Z axis, spreading evenly on the X-Y plane in S'. The bar array travels in the X direction in parallel with the X-Y plane. The viewer is located at a fixed distance away on the positive Z axis in S, and looks towards the X-Y plane. This can be seen as a 3D extension to the 2D light grid considered by Scott and Viner[30]. Our results are shown in figure (7), (8), (9), (10), (11) and (12).

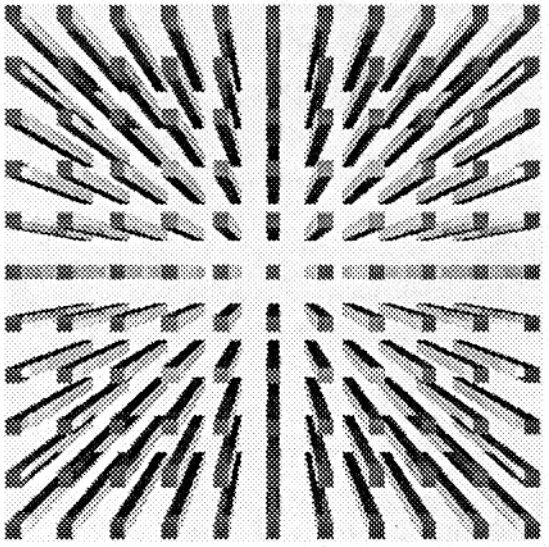

Figure 7: Array of bars viewed at β = 0.0 (©1989 Hsiung, Dunn & Loofbourrow)

The apparent hyperbolic shapes described in [30] are distinct in these figures. It is worth noting that in [30], orthographic projection was employed in forming images. The ray-tracing technique, however, gives us the capability to produce a perspective projection of the objects modeled. This is a more accurate representation of the object space.

In the third set of experiments, we ray-traced a lattice in Spacetime (figure (13)). The lattice consists of intersecting perpendicular rods with small spheres situated at each point of intersection.[10] The observer is outside of this lattice and travels "into" the lattice.[11] Images from several different viewing directions are produced (three such directions are shown in figure (13)). The relative speed of motion is varied to explore the non-intuitive aspects of visualizing Special Relativity effects. The images are shown in the following figures:

- Figure (14): The lattice; stationary with respect to the viewer. The viewer looks forward (direction 1 in figure (13)).
- Figure (15): The lattice at 0.5c. The viewer looks forward.
- Figure (16): The lattice at 0.9c. The viewer looks forward.
- Figure (17): The lattice at 0.99c. The viewer looks forward.
- Figure (18): The lattice at 0.5c with the viewer looking up at a 45° angle (direction 2 in figure (13)).
- Figure (19): The lattice at 0.5c with the viewer looking up and to the right at 45° respectively.

[9] with a meter stick, on the rendered images.

[10] We were inspired by the lattice-clock in [32] and the intriguing roller-coaster structure in amusement parks.

[11] Relatively speaking. In our simulations, it is always the objects (in S') that travel.

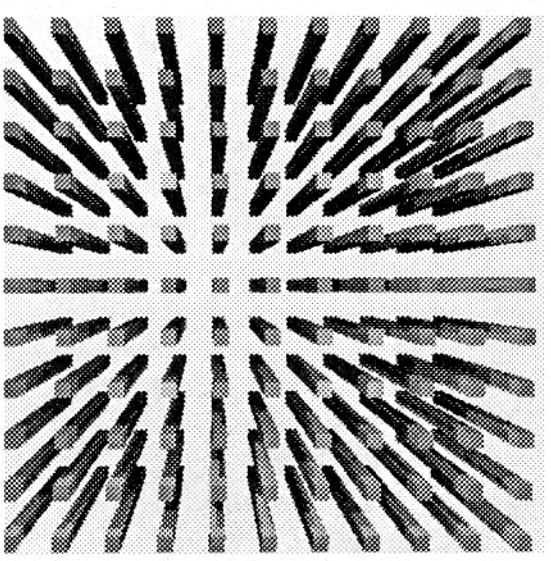

Figure 8: Array of bars viewed at β = 0.1 (©1989 Hsiung, Dunn & Loofbourrow)

3.3 Verification and discoveries

The apparent relativistic effects from the second and third set of experiments are described below.

3.3.1 Array of bars

At relativistic speeds, each individual bar of the array aggregate undergoes a distortion in the perpendicular direction[12] that can be described as a non-homogeneous shear. This distortion contributes to the hyperbolic curvature displayed by the outline of the entire array, which can be taken as a cubic structure in S' space. The array elements also *appear* rotated away from the direction of motion, making the sides visible to the observer. Both the shearing and the rotation are results of the simultaneous arrival of light emitted at different past times from different parts of the bodies. The Lorentz-Fitzgerald Contraction in the direction of motion is also apparent. Traveling near the speed of light, the array is seen squeezed as well as rotated.

[12] with respect to the bar body orientation.

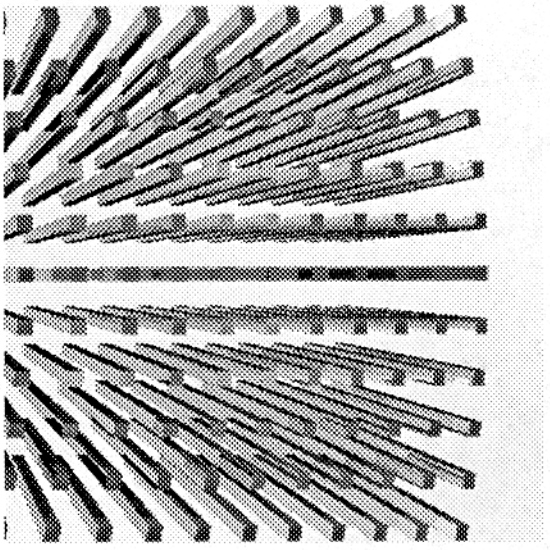

Figure 9: Array of bars viewed at β = 0.5 (©1989 Hsiung, Dunn & Loofbourrow)

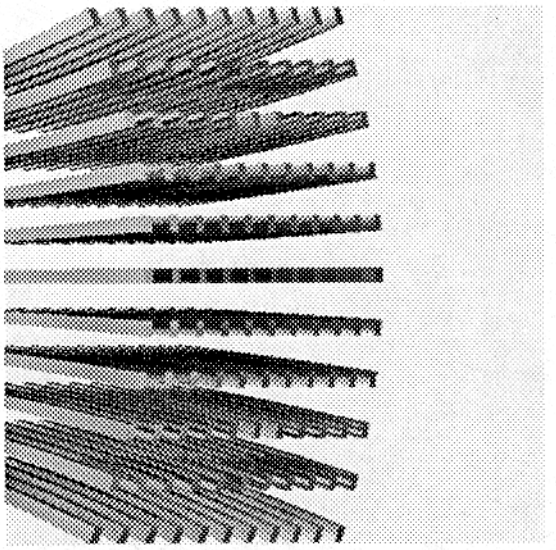

Figure 10: Array of bars viewed at β = 0.9 (©1989 Hsiung, Dunn & Loofbourrow)

3.3.2 Latticework

In the lattice experiments, some observed effects are as follows:

1. The Lorentz-Fitzgerald contraction effect in the direction of motion produces the apparent foreshortening of the lattice in the images. This effect is most marked in the illustrations at 0.9 and 0.99 times the speed of light.
2. The Doppler effect appears as a lens-like effect. This is especially prominent in the off-center portion of each image, which is formed by light rays that reach the image plane at an angle off of the direction of travel. The finite time-of-flight for rays to reach the image plane from the objects requires each ray registered on the image plane to come from a different past in time. The off-centered rays (corresponding to the off-centered image pixels) come from more remote pasts in time than the central rays and render the off-centered objects as being distorted away from the viewer.

In all of the above lattice simulations, we chose the view time of the imaging event[13] in each trace to be such that the event [0, 0, 0, 0] (in both S and S') always shows up at the center of each image plate. This explains the similarity in size of the four frontal central spheres in imagery produced from varying speeds. These four spheres are very close to the spatial point $(0, 0, 0)_{S'}$, which is at their geometric center.

4 Discussion

4.1 Possible extensions

Our implementation is self-contained but preliminary. In its present form, it has the following simulation limitations:[14]

- The light sources are static in space and time.[15] A more complete light source model should incorporate moving light sources, self luminous bodies, and/or sources that change the illumination nature — such as pulsed illumination or the "radar world"[40][20]. The latter suggests a practical *active* image generation process in which the observer possesses the only (or major) radiation energy source in Spacetime and sends out radiation beams in order to "see" the environment.
- The relative motion of S and S' is one dimensional and linear. The following generalization to our implementation is essential in order to simulate more realistic and dynamic scenes:
  - *3D* relative motion of objects and viewer. The general Lorentz Transformation is required to formulate the ray transformation between frames.
  - Multiple velocity system; objects move with different directions and speed relative to the viewer.
  - Angular motion. In this case, points on the surface of a rotating object experience different linear velocities relative to the viewer. The visual result of such motion is difficult to conceive.
- We have not implemented texture mapping — an element necessary, for example, to show surface feature distortion effects on a fast moving planet.
- The relativistic Doppler frequency shift is not modeled, nor are the effects of the participating media for light propagation (the atmospheric effects).

[13] The *imaging event* is the Spacetime event with spatial coordinates of the viewpoint and time coordinate of the view time.

[14] Some of the extensions have been completed since the submission of this paper. Specifically, 3D relative motion, multiple velocity system and relativistic Doppler frequency shift have been implemented and will be reported elsewhere.

[15] In either S or the S'.

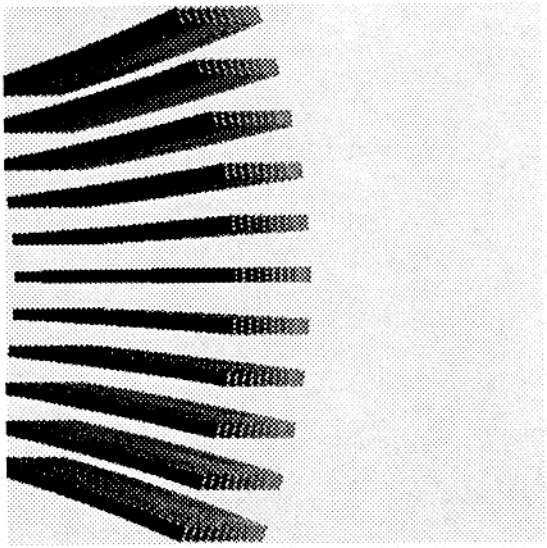

Figure 11: Array of bars viewed at $\beta = 0.99$ (©1989 Hsiung, Dunn & Loofbourrow)

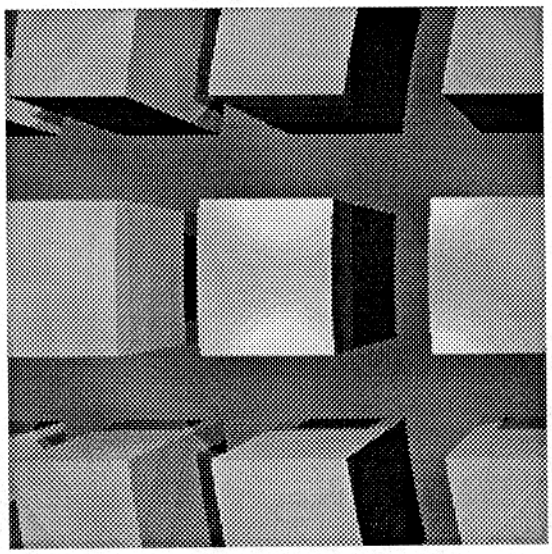

Figure 12: Zoom-in of array of bars viewed at $\beta = 0.5$ (©1989 Hsiung, Dunn & Loofbourrow)

4.2 Multiple velocity intersection

In the more general case in which objects are moving at different velocities, it is impossible to find a single frame in which all objects are stationary (the S' frame as defined above). Every object definition carries a velocity parameter in the S frame which in turn defines the path that the object travels in Space-time. For each ray, the intersection test against every object can be conducted in the particular frame in which the object is stationary. A sorting of the intersection *times* in the S frame can then be employed to identify the true visible event (and the associated frame). The secondary rays resulting from a hit may be generated in that frame by the correct application of the classical laws of optics.

4.3 Importance of this research

The significance of our work is twofold: (1) It fills in a void in past research and significantly advances the historical quest to visualize Special Relativity effects. (2) It promises to bring forth a new level of comprehension to Special Relativity. We elaborate on both points in the following.

Through the application of state-of-the-art computation technology and simulation techniques to earlier work in Physics, we have developed a generalized simulation approach to visualize the relativistic world with a global illumination model that:

- incorporates the *correct* and *complete* natural optical phenomena for perspective projection, reflection, refraction and shadow casting.
- unifies the *ad hoc* viewing conditions of previous attempts into one integrated treatment. We overcome the earlier limitations of a single pulse source or single self-luminous object by applying multiple light sources that produce a homogeneous and static environment of illumination. The viewing conditions are flexible due to our ray-tracing implementation.

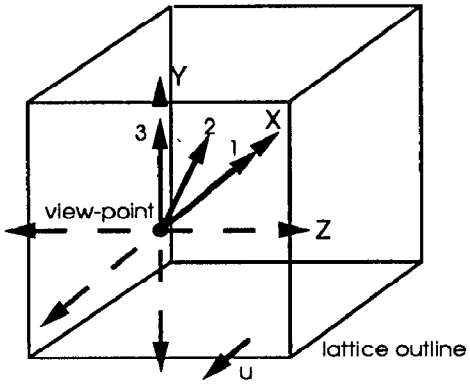

Figure 13: Setup for lattice traces

REST-frame, therefore, gives a closer approximation to the *real* physical world in which we exist, and fills in the details that were missing or were interpolated in the earlier mathematical manipulations. The variation of viewing orientation given to the observer in this context allows the observer a greater complexity of perception than in any previous model.

Having created this approach, and with the hope of illuminating the extent of its future, we state the following:

1. The power of this work lies in its ability to bring out and demonstrate, in simulated environments, broader implications of the laws of Special Relativity.

2. Simulated relativistic perceptual observations will reveal many aspects of the non-intuitive world which will eventually be incorporated into everyday reality. A paradigm of new working intuition will evolve based on these simulations.

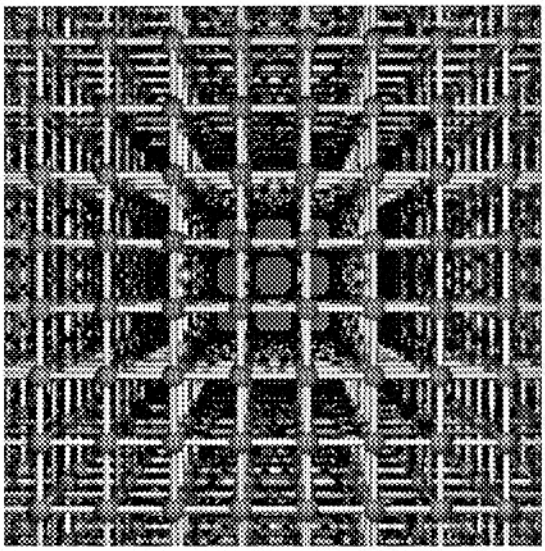

Figure 14: Lattice viewed at $\beta = 0.0$ (©1989 Hsiung, Dunn & Loofbourrow)

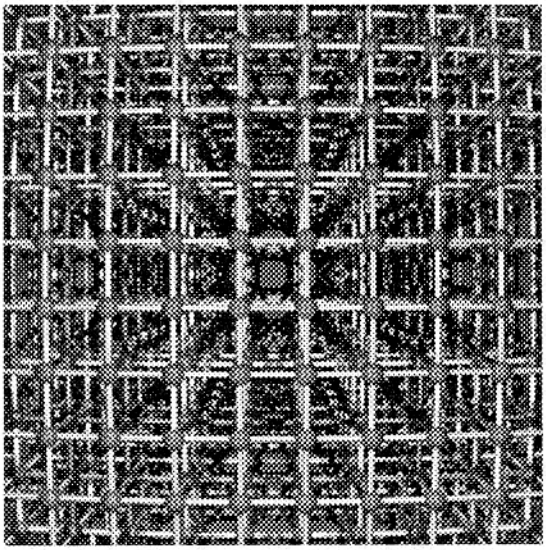

Figure 15: Lattice viewed at $\beta = 0.5$ (©1989 Hsiung, Dunn & Loofbourrow)

5 Conclusion and future work

The REST-frame algorithm is a construct used for the study of nature. It is a new analytical tool which moves beyond the root mathematical language by means of an interactive exploratory visualization methodology. It creates an environment for empirical simulation. The fields of education and research in cosmology, nuclear science, space science and exploration, cognitive science and perceptual studies, computer micro-architecture and networks, and interdisciplinary design science may benefit from the visualization tools and techniques we have developed. Further work may involve the simulation of visual effects in accelerated frames of reference and animation studies of macroscopic and microscopic domains. Our visualization methodology is a preliminary step leading to further advances in attuning human experimental or experiential senses of the world and the visionary capacity of the mind with far reaching abstract mathematical descriptions. The enhanced stimulation of the visual sensibility and imagination contributes to the evolution of new forms of visual language and intuition which deepen the appreciation and participation of humanity in the environment of universe.

Acknowledgments

We would like to thank Nathan Loofbourrow for his assistance in preparing ray-tracing images and for insightful discussions that contributed to this presentation. We are also grateful to Dr. Robert H. Thibadeau for his continuous advice and support. Also we thank Alison Peters for her timely assistance.

References

[1] John Amanatides. Realism in computer graphics: a survey. *IEEE Computer Graphics and Applications*, 44, Jan 1987.

[2] B. Arnaldi, T. Priol, and K. Bouatouch. A new space subdivision method for ray tracing CSG modelled scenes. *Visual Computer*, 3:98–108, 1987.

[3] J. Arvo and D. Kirk. Fast ray tracing by ray classification. *Computer Graphics (SIGGRAPH)*, 55–64, July 1987.

[4] Jim Arvo and David Kirk. A survey of ray tracing acceleration techniques. In *ACM SIGGRAPH '88 Course Notes*, SIGGRAPH '88, July 1988.

[5] H. A. Atwater. Apparent distortion of relativistically moving objects. *Journal of the Optical Society of America*, 52(2):184–7, Feb 1962.

[6] Ronen Barzel and Alan H. Barr. A modeling system based on dynamic constraints. *Computer Graphics (SIGGRAPH)*, 179, 1988.

[7] J. Cleary and G. Wyvill. Analysis of an algorithm for fast ray tracing using uniform space subdivision. *Visual Computer*, 4:65–83, July 1988.

[8] R. Cook and K. Torrance. A reflectance model for computer graphics. *ACM Trans. Graphics*, 1(1):7–24, Jan 1982.

[9] Robert L. Cook, Thomas Porter, and Loren Carpenter. Distributed ray tracing. *Computer Graphics*, 1803:137–145, July 1984.

[10] Mark Dippe and John Swensen. An adaptive subdivision algorithm and parallel architecture for realistic image synthesis. *Computer Graphics (SIGGRAPH)*, 149–158, July 1984.

[11] A. Fujimoto, T. Tanaka, and K. Iwata. ARTS: accelerated ray-tracing system. *IEEE Computer Graphics and Applications*, 16–26, April 1986.

[12] George Gamow. Remarks on Lorentz contraction. *Proceedings of the Natural Academy of Science*, 47:728–9, March 1961.

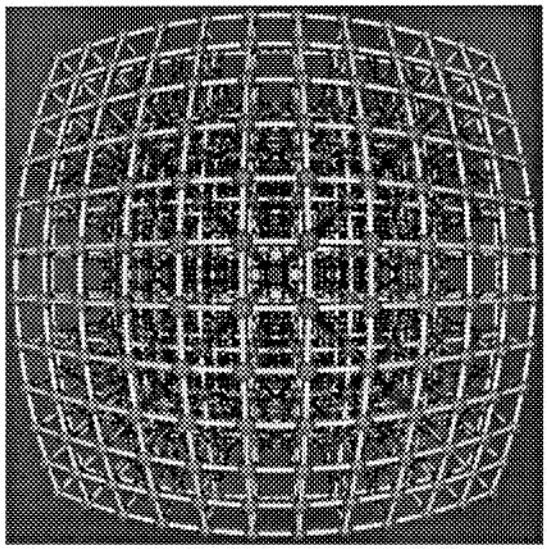

Figure 16: Lattice viewed at $\beta = 0.9$ (©1989 Hsiung, Dunn & Loofbourrow)

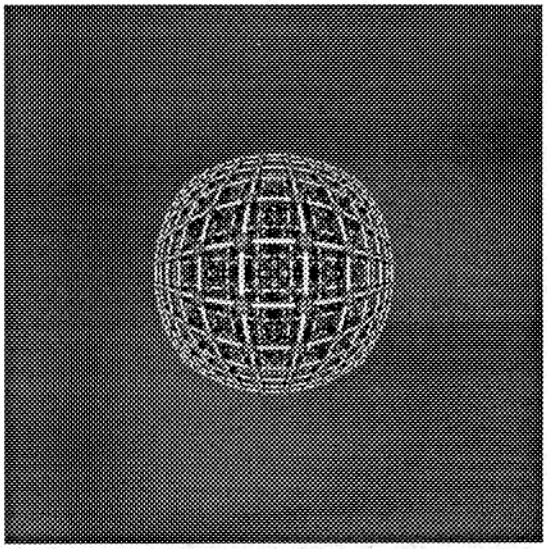

Figure 17: Lattice viewed at $\beta = 0.99$ (©1989 Hsiung, Dunn & Loofbourrow)

[13] A. S. Glassner. Space subdivision for fast ray tracing. *IEEE Computer Graphics and Applications*, 15–22, October 1984.

[14] A. S. Glassner. Spacetime ray tracing for animation. *IEEE Computer Graphics and Applications*, 60–70, March 1988.

[15] R. Goldstein and R. Nagel. 3-D visual simulation. *Simulation*, 25, 1971.

[16] Ping-Kang Hsiung. Accelerating ARTS. *Thesis Proposal, Carnegie Mellon University*, Feb. 1989.

[17] T.L. Kay and J.T. Kajiya. Ray tracing complex scenes. *Computer Graphics (SIGGRAPH)*, 269–278, Aug. 1986.

[18] H. Kobayashi, S. Nishimura, H. Kubota, T. Nakamura, and Y. Shigei. Load balancing strategies for a parallel ray-tracing system based on constant subdivision. *Visual Computer*, 4:197, 1988.

[19] C. Møller. *The Theory of Relativity*. Oxford University Press, 1960.

[20] N. C. McGill. The apparent shape of rapidly moving objects in special relativity. *Contemporary Physics*, 9(1):33–48, 1968.

[21] H. Niimi, Y. Imai, M. Murakami, S. Tomita, and H. Hagiwara. A parallel processor system for three-dimensional color graphics. *Computer Graphics (SIGGRAPH)*, 18(3):67, July 1984.

[22] H. Nishimura, H. Ohno, T. Kawata, I. Shirakawa, and K. Omura. Links-1: a parallel pipelined multimicrocomputer system for image creation. In *Proceedings 10th Symp. Computer Architecture (SIGARCH 83)*, page 387, ACM, New York, 1983.

[23] M. Ohta and M. Maekawa. Ray coherence theorem and constant time ray tracing algorithm. In *Computer Graphics 1987*, page 303, Springer-Verlag, 1987.

[24] R. Penrose. The apparent shape of a relativistically moving sphere. *Proceedings of the Cambridge Philosophical Society*, 55:137–9, July 29 1958.

[25] Bui Phong. Illumination for computer generated pictures. *CACM*, 18(6):311, June 1975.

[26] Robert Resnick. *Introduction to Special Relativity*. Rensselaer Polytechnic Institute, 1968.

[27] W. Rindler. Length contraction paradox. Jan 29 1961.

[28] H. Sato, M. Ishii, K. Sato, M. Ikesaka, H. Ishihata, M. Kakimoto, K. Horota, and K. Inoue. Fast image generation of constructive solid geometry using a cellular array processor. *Computer Graphics (SIGGRAPH)*, 19(3):95–102, July 1985.

[29] G. D. Scott and H. J. van Driel. Geometrical appearances at relativistic speeds. *American Journal of Physics*, 38(8):971–7, August 1970.

[30] G. D. Scott and M. R. Viner. The geometrical appearance of large objects moving at relativitic speeds. *American Journal of Physics*, 18(2):109–144, Jan 1965.

[31] C. W. Sherwin. Regarding the observation of the Lorentz contraction on a pulsed radar system. *American Journal of Physics*, 29(2):67–9, Feb 1961.

[32] E. Taylor and J. Wheeler. *Spacetime Physics*. M.I.T. / Princeton, 1966.

[33] J. Terrell. Invisibility of the Lorentz contraction. *Physical Review*, 116(4):1041, 1959.

[34] Demetri Terzopoulos, John Platt, Alan Barr, and Kurt Fleischer. Elastically deformable models. *Computer Graphics (SIGGRAPH)*, 205, 1987.

[35] K. E. Torrance and E. M. Sparrow. Theory for off-specular reflection from roughened surfaces. *Journal of the Optical Society of America*, 1105, 1967.

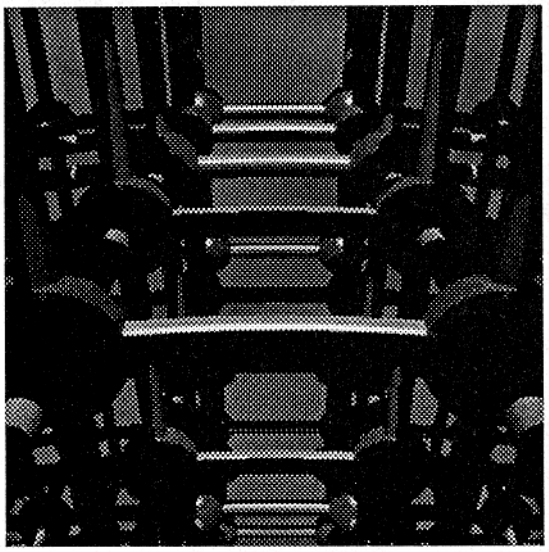

Figure 18: Lattice viewed at 45° upward at $\beta = 0.5$ (©1989 Hsiung, Dunn & Loofbourrow)

[36] V.F. Weisskopf. The visual appearance of rapidly moving bodies (section). *Physics Today*, 13(9):24, 1960.

[37] T. Whitted. An improved illumination model for shaded display. *CACM*, 343–349, June 1980.

[38] Andrew Witkin, Kurt Fleischer, and Alan H. Barr. Energy constraints on parameterized models. *Computer Graphics (SIGGRAPH)*, 225, 1987.

[39] Andrew Witkin and Michael Kass. Spacetime contraints. *Computer Graphics (SIGGRAPH)*, 159, 1988.

[40] Sten Yngström. Observation of moving light-sources and objects. *Arkiv för Fysik*, 367, 1962.

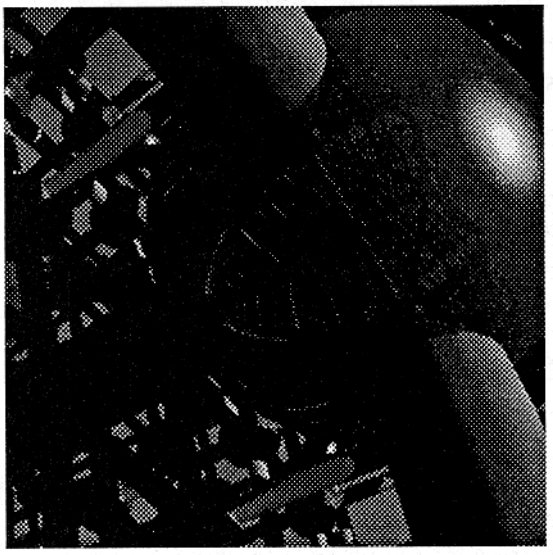

Figure 19: Lattice viewed at 45° upward and sideways at $\beta = 0.5$ (©1989 Hsiung, Dunn & Loofbourrow)